Astron. Astrophys. 317, 65–72 (1997)

ASTRONOMY
AND
ASTROPHYSICS

Dust and molecules in the Local Group galaxy NGC 6822

II. CO and molecular hydrogen

F.P. Israel

Sterrewacht Leiden, P.O. Box 9513, 2300 RA Leiden, The Netherlands

Received 6 September 1995 / Accepted 24 February 1996

Abstract. Emission from the J=1-0 ^{12}CO transition was detected unambiguously at 4 out of 17 observed positions in the Magellanic irregular galaxy NGC 6822; two more positions yielded marginal 3σ detections. These positions include the HII region complexes Hubble V and Hubble I/III, and two IRAS far-infrared emission peaks not associated with bright HII regions. The bright HII region Hubble X was not detected. The CO emission detected is rather weak, typically 0.4 - 0.8 K km s^{-1} in a 105 pc beam. It is well-correlated with infrared brightness, but not with that of HI emission.

The sum of all observed spectra yields an integrated CO signal I_{CO} = 6.4$\pm$1.2 K km s^{-1}, 70% greater than the sum of the individual detected components. This implies the presence of more widespread weak CO emission not detected in individual pointings. The total CO content of NGC 6822 is argued to be 1.2 (+1.2, -0.6) $\times$ 10^5 K km s^{-1} pc^2, nominally twice the amount detected.

The available HI, infrared and CO data have been used to estimate the magnitude of the empirical conversion factor X = N(H$_2$)/I_{CO} in NGC 6822, resulting in X_{N6822} = 8$\pm$3 $\times$ 10^{21} cm^{-2} (K km s^{-1})$^{-1}$, or 40$\pm$15 times higher than the Galactic conversion factor. Even with this factor, the total H$_2$ mass of NGC 6822 is estimated at only M(H$_2$) = 1.5 (+3, -1) $\times$ 10^7 M$_\odot$, roughly 15 per cent of the HI mass.

In the Galactic foreground, CO emission from a diffuse cloud was detected with a narrow linewidth of about 1 km s^{-1} at V_{LSR} = +5 km s^{-1}.

Key words: galaxies: individual: NGC 6822 – galaxies: ISM; irregular; Local Group – radio lines: galaxies

1. Introduction

NGC 6822 (DDO 209) is a Local Group dwarf irregular galaxy of the Magellanic type (IB(s)m). It is located at a distance of 500 kpc (McAlary et al. 1983). In its properties, it resembles the Magellanic Clouds. Its total mass is 1.5 $\times$ 10^9 M$_\odot$, while its HI mass is between 1 and 1.5 $\times$ 10^8 M$_\odot$ (Volders & Högbom 1961; Fisher & Tully 1975; Gottesmann & Weliachew 1977). The optical aspect of NGC 6822 is that of a bar dominated by an irregular distribution of OB associations (Wilson 1992b and references therein) and HII regions (Hodge, Kennicutt & Lee 1988). Major OB associations, as well as the large and bright HII regions Hubble I, III, V and X (Hubble 1925) are found at the northern end of the bar.

Despite its large number of mostly minor HII regions, NGC 6822 is not very active in forming stars (*cf.* Gallagher et al. 1991; Hodge 1980; Vangioni-Flam et al. 1980). In a recent paper, we derived a star formation rate averaged over the last 10^7 years of dM/dt = 0.04 M$_\odot$ yr^{-1} and an area-normalized star formation rate of dM/(dt dA) = 0.013 M$_\odot$ yr^{-1} kpc^2, rather low for star-forming dwarf galaxies, but comparable to the area-normalized star formation rates of disk galaxies (Israel, Bontekoe & Kester 1995). The relatively low metal abundance of its HII regions ([O/H] = 1.7 $\times$ 10^{-4}: Lequeux et al. 1979; Pagel, Edmunds & Smith 1980; Skillman, Terlevich & Melnick 1989) is consistent with a relatively low time-averaged star formation rate. This abundance is about one third that of the Solar Neighbourhood ([O/H] = 5 $\times$ 10^{-4}) and between those given by Dufour (1984) for the LMC ([O/H] = 2.7 $\times$ 10^{-4}) and the SMC ([O/H] = 1.1 $\times$ 10^{-4}). Also consistent with a relatively low present star formation rate in NGC 6822 is its low level of radio continuum emission (Klein, Gräve & Wielebinski 1983). The total radio luminosity of NGC 6822 is less than that of the single brightest HII region NGC 604 in M33. NGC 6822 has a dust-to-gas ratio of the order of 1.4 $\times$ 10^{-4} (Israel, Bontekoe & Kester 1995), which is well within the range generally found for dwarf galaxies.

NGC 6822 is a weak CO emitter. Early attempts by Elmegreen, Elmegreen & Morris (1980) to detect CO emission from various positions in NGC 6822 failed to yield a signal above T_{mb} = 120 mK in a 65$''$ beam. Observations by Wilson (1992a), in a 55$''$ beam, yielded three detections out of 47 positions observed. Observations at 15$''$ resolution by Ohta et al. (1993) of Hubble V yielded a detection at a single position out of three observed.

Send offprint requests to: F.P. Israel

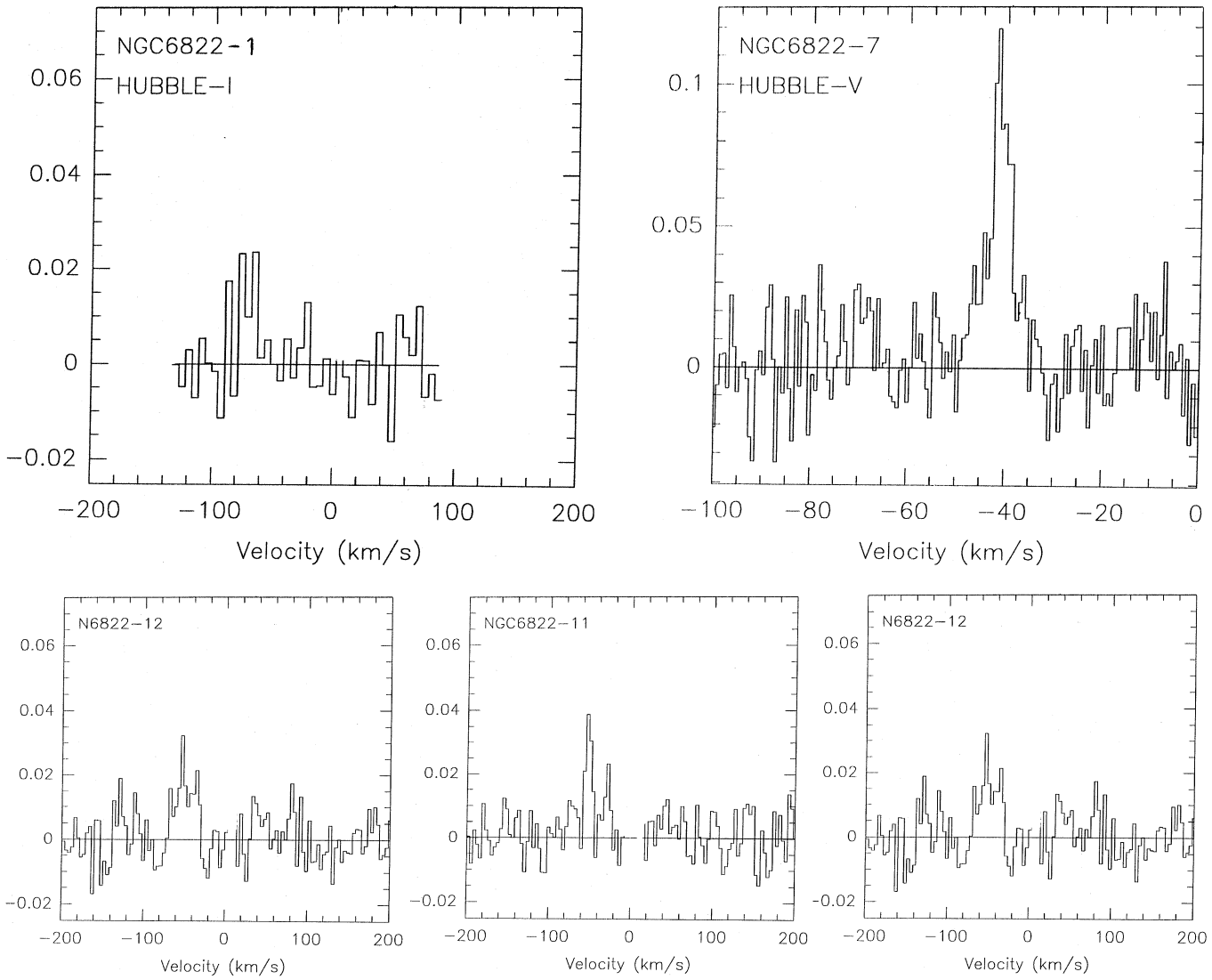

Fig. 1. Observed CO spectra; numbers refer to Table 1. Intensities are given in units of T_A^* and can be converted to T_{mb} by dividing them by 0.7. Spectra are binned to a velocity resolution of 3.6 km s^{-1}, except those of Hubble I and Hubble V which are binned to resolutions of 5.4 km s^{-1} and 0.7 km s^{-1} respectively. Residual emission due to the Galactic foreground line at +5 km s^{-1} (see Sect. 3.1) has been removed.

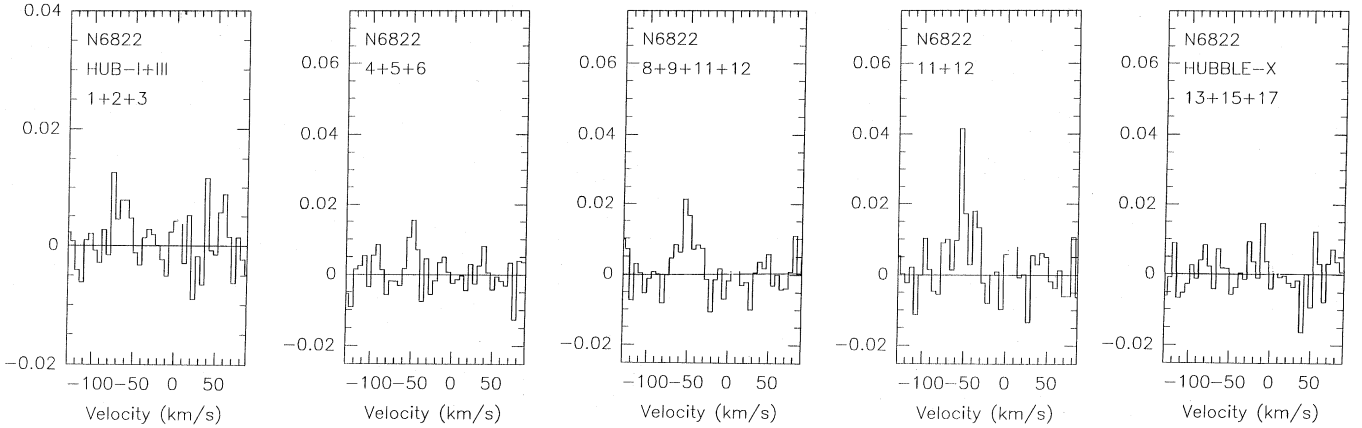

Fig. 2. Averaged CO spectra; numbers refer to Table 1. Intensities are given in units of T_A^*. Spectra are binned to a velocity resolution of 5.4 km s^{-1}. Residual emission due to the Galactic foreground line has been removed.

Table 1. SEST observations of J=1-0 ^{12}CO in NGC 6822

Position	α(1950) $h\ m\ s$	δ(1950) $^\circ\ '\ ''$	t_{int} (min)	T_{mb} (mK)	ΔV (km s^{-1})	V_{LSR} (km s^{-1})	$\int T_{mb} dV$ (K km s^{-1})	Associated HII Region
1	19 41 42.0	-14 49 17	140	(23±8	17±6	-68±3	0.39±0.12)	Hubble I
2	41 43.2	49 27	200	<22	—	—	<0.40	
3	41 44.4	49 38	180	<15	—	—	<0.40	Hubble III
4	41 53.0	59 42	100	<29	—	—	<0.20	
5	41 59.1	59 55	180	41±6	21±5	-50±2	0.80±0.14	Ho 18; HK 30
6	42 03.0	59 35	132	<41	—	—	<0.34	Ho 10; HK 56
7	42 03.2	50 28	300	157±23	6±1	-41±1	0.77±0.07	Hubble V
8	42 07.0	55 06	120	(50±23	8±3	-51±2	0.44±0.16)	HK 66/67
9	42 07.2	55 45	100	<55	—	—	<0.45	Hodge 12
10	42 07.3	50 29	180	<23	—	—	<0.33	
11	42 08.0	55 09	160	62±15	7±2	-53±1	0.48±0.09	KD 24
12	42 09.2	54 51	200	32±9	27±3	-50±4	0.90±0.16	KD 24
13	42 11.4	50 30	20	<45	—	—	<0.40	HK 73
14	42 13.5	53 00	120	<20	—	—	<0.41	
15	42 15.6	50 31	300	<21	—	—	<0.25	Hubble X
16	42 15.8	-15 04 42	100	<55	—	—	<0.50	KD 27
17	42 19.7	-14 50 32	180	<30	—	—	<0.50	
Averaged spectra								
1+2+3	.....	.....	520	(14±6	22±4	-68±3	0.33±0.06)	Hubble I + III
4+5+6	.....	.....	412	(26±9	11±3	-49±2	0.30±0.09)	
8+9	.....	.....	220	(51±14	6±3	-52±1	0.34±0.10)	
8+11	.....	.....	280	59±11	9±2	-52±1	0.57±0.11	
11+12	.....	.....	360	30±10	27±6	-51±3	0.86±0.19	
8+9+11+12	.....	.....	580	43±10	26±7	-51±4	0.69±0.19	
13+15+17	.....	.....	500	<20	—	—	<0.30	Hubble X
Summed Spectra								
All LRS	.....	.....	1420	130±22	38±6	-51±3	4.7±0.6	area: 9 beams
All HRS	.....	.....	2712	148±31	44±9	-54±5	6.4±1.2	area: 15 beams

In this paper we present new CO observations of NGC 6822. Together with the results from an analysis of the infrared emission of the galaxy (Israel, Bontekoe & Kester 1995, hereafter Paper I), these are used to further study the molecular hydrogen component of the interstellar medium in this galaxy. NGC 6822 is of interest, because its membership of the Local Group allows us to study both the global and the detailed distribution of its gas and dust.

2. Observations and data handling

All observations were made in two runs (March 1989 and March 1990) with the SEST 15 m telescope [1] The telescope has a FWHM beamsize of 43″ at the operating frequency of 115 GHz, and a main-beam efficiency $\eta_{mb} = 0.71$. During the observations, the overall system temperature including the sky varied between 750 and 650 K. The observations were made in a double-beam-switching mode with a throw of 12′, well clear of the galaxy. The March 1989 observations were all made with the high-resolution AOS backend at SEST. This backend provided a bandwidth of 86 MHz (224 km s^{-1}) with 2000 channels of separation 80 kHz (velocity resolution 0.21 km s^{-1}). During the March 1990 run, we used the same backend, as well as the low-resolution backend in parallel. That backend provided a useful bandwidth of 0.5 GHz (1300 km s^{-1}) with 720 channels of separation 0.7 MHz (velocity resolution 3.6 km s^{-1}).

As we noticed imperfectly cancelled Galactic foreground CO emission at V_{LSR} = +5 km s^{-1} (as well as telluric emission at +41 km s^{-1}), we also obtained frequency-switched spectra towards four positions, observed with a throw of 15 MHz in order

[1] The Swedish-ESO Submm Telescope (SEST) is operated jointly by the European Southern Observatory (ESO) and the Swedish Science Research Council (NFR).

Table 2. Observed line parameters of Galactic foreground CO

Position	l	b	T_{mb}	ΔV	V_{LSR}
	°	°	(mK)	(km s^{-1})	(km s^{-1})
1	25.4	-18.3	1630±45	0.75	+4.9
6	25.3	-18.4	970±85	1.25	+5.4
7	25.4	-18.4	1000±70	1.15	+5.3
15	25.5	-18.4	700±140	0.80	+5.1

to determine the line parameters of this emission. Integration times varied from 45 to 105 minutes. Because the frequency-switched spectra suffered from relatively poor baselines, we did not use this technique on the weak CO emission from NGC 6822 itself. Neither the Galactic foreground line nor the telluric line interferes with the CO emission from NGC 6822 which occurs at lower velocities.

The SEST CO results are given in Table 1. Detections are illustrated in Fig. 1. Because of the low antenna temperatures and narrow linewidths characterizing the CO emission from NGC 6822, total integration times (source + reference) ranged from 90 minutes to 5 hours. In order to search for very weak emission, we have also, wherever feasible, coadded data obtained towards positions differing less than two beams in pointing and used these to construct the integration-time weighted average spectra, shown in Fig. 2. Finally, we have coadded all spectra obtained in the low-resolution and in the high-resolution backends respectively and used these to constructe sum-spectra (equal weight per observed position) in order to obtain an estimate of the total CO content of the galaxy. All spectra were binned to various degrees in order to determine whether emission was present. Only linear baselines were subtracted.

3. Analysis

3.1. Galactic foreground

As mentioned in the previous section (see also Wilson 1992a, her Fig. 2a), Galactic foreground CO emission is seen towards most if not all of NGC 6822. This foreground is present in the form of a narrow line at V_{LSR} = +5 km s^{-1}. We obtained frequency-switched spectra towards Hubble I, Hubble V, Hubble X and infrared source 4 in the bar of NGC 6822. The results are given in Table 2. The line is typically 1 K and varies in strength by a factor of two. The distance of the emitting cloud is uncertain; only an upper limit can be derived. The Galactic rotation model with R_o = 8.5 kpc formally yields a near distance of 860 pc for the observed radial velocity V_{LSR} = +5 km s^{-1}, corresponding to a distance z = 290 pc to the Galactic plane at the observed latitude b = -18.4°. If we take into account a cloud-cloud velocity dispersion of 8 km s^{-1}, we conclude that the foreground cloud must be closer than 1.3 kpc, and be closer to the Galactic plane than 450 pc. Actual distances may be much less than this.

As the lines are almost, but not completely, canceled in the beam-switched spectra obtained by offsetting 12′ in azimuth, they must arise in a cloud complex of 30′ or more in size. This extent corresponds to 8.7 × d pc, where d is the true distance in kpc.

The narrow linewidth (typically 1 km s^{-1}) is remarkable and suggests that the emission arises in a tenuous, translucent cloud. The line parameters in Table 2 are very similar to those of diffuse high-latitude clouds observed by Gredel et al. (1992, 1994) and especially those observed by Stark (1993). These clouds have low optical depths even in ^{12}CO, and estimated molecular hydrogen column densities each of order a few times 10^{20} cm^{-2}, corresponding to visual extinctions typically in the range A_V = 0.1 - 0.5 mag. This is just consistent with the variable foreground absorption towards NGC 6822 A_V = 0.6 - 2.1 mag (Hodge 1977; Humphreys 1980; Wilson 1992b).

We have compared the detected CO line strengths to the HI profile in a 35′ beam (Hartmann 1994) in the direction of NGC 6822. Although this beam is much larger than the SEST beam, the comparison is not without merit in view of the extent of the CO emission, and the relatively small variation in intensity towards NGC 6822 and the reference positions. The CO cloud has strong HI emission blended with the zero-velocity peak; this HI feature shows a significant velocity gradient on a scale of a degree or so. IRAS survey maps show very extended, but weak Galactic foreground cirrus emission which smoothly blends with the extended infrared emission from NGC 6822 itself.

3.2. CO emission from NGC 6822

3.2.1. Correlation with HII regions and infared sources

The positions listed in Table 1 represent samplings of five distinct regions in NGC 6822. Positions 1, 2 and 3 sample the HII region complex Hubble I/Hubble III in the northeast of NGC 6822. It is a moderately strong, extended infrared source (No. 2, Paper I). A marginal (3σ) detection was obtained towards Hubble I, within 6 km s^{-1} from the HI velocity at this position (Gottesman & Weliachew 1977). The line is relatively broad with ΔV = 17 km s^{-1}. The CO upper limit given by Wilson (1992a, hereafter W92) for this position is consistent with the weak signal from this object. The coadded spectra (Table 1, Fig. 2) yield a higher CO luminosity for the Hubble I/Hubble III complex indicating the presence of relatively weak but extended CO emission.

The second set of positions (7, 10, 13, 15, 17) is spaced about 1′ (145 pc) apart. It samples a line through and including the major HII regions Hubble V and Hubble X in the north of NGC 6822. Both are strong infrared emitters (No.'s 5 and 8, Paper I). The highest CO peak intensity was observed at position 7 towards Hubble V, also detected in CO by W92 and Ohta et al. (1993). Comparison of the detected line strengths and the relevant beam areas suggests that the extent of CO associated with Hubble V is somewhat smaller than the SEST beam of 43″. Whereas Hubble X was detected by W92, we only obtained an upper limit at position 15. Given the differences in beamsize (55″ versus the 43″ beam of the SEST), the nominal centering of the beams ($\Delta\theta$ = 11″) and the pointing uncertainties of the

W92 survey (15″), the results of both surveys are consistent if the CO cloud associated with Hubble X is located some 20″ to the east-southeast of position 15.

The third set of positions (4, 5 and 6) sample a strong, relatively compact infrared source (No. 4, Paper I) in the southern part of the NGC 6822 bar. It coincides with a major HI maximum (Gottesman & Weliachew 1977), but only minor HII regions are found in this direction (Hodge, Kennicutt & Lee 1988). CO was clearly detected at position 5 at a velocity within 5 km s^{-1} of the HI velocity. No CO was detected at positions 4 and 6 offset by 90″ (215 pc) west and 60″ (145 pc) east respectively. Coadding the spectra from positions 4, 5 and 6 does not yield a luminosity higher that that of position 5 alone. In the same part of NGC 6822, W92 detected CO emission 70″ (170 pc) northwest of position 5, but at a velocity 40 km s^{-1} more negative than that of our detection.

The fourth region, sampled by positions 8, 9, 11 and 12, coincides with a strong and somewhat extended infrared maximum (No. 6, Paper I) in the central part of the NGC 6822 bar. The maps by Gottesman & Weliachew (1977) show a relatively weak extension of HI contours from the above-mentioned strong maximum towards the infrared source. We detected CO emission at positions 11 and 12, while position 8 yielded a marginal (3σ detection). Beam overlap between positions 8, 9 and 12 is very little, but the beam centered on position 11 overlaps with those centered on positions 8 and 12. The emission from positions 8 and 11 has a modest velocity width of 8 km s^{-1}, whereas position 12 shows a rather broad line with a width of 27 km s^{-1}. The spectra in Fig. 1 suggest that this large linewidth is due to the blending of two or three narrower CO components at slightly different velocities, but the signal-to-noise ratio is not good enough to be certain of this. The results suggest that the detected CO emission is extended over more than 20″, which is supported by the coadded result (Table 1, Fig. 2). We also sampled a position (#14) halfway between this region and Hubble X, yielding only an upper limit. None of these positions was observed by W92.

The final region, likewise not observed by W92, was sampled by position 16. It is located in the southwest of NGC 6822 and coincides with a strong HI maximum, but relatively weak infrared emission (Paper I). No CO was detected.

The observed integrated CO brightnesses I_{CO} are well-correlated with the FIR luminosities of the corresponding infrared sources. When the latter are normalized to the same dust temperature T_d = 30 K, the relation between the two quantities is empirically approximated by $I_{CO} = 2.5 \times 10^{12}$ FIR′ (K km s^{-1}) (W^{-1} m^2), where FIR′ is the temperature-normalized far-infrared luminosity. We have concluded in Paper I that the infrared emission is not well-correlated with HI, nor with thermal radio continuum emission unless sources are separated according to the nature of their heating sources. Indeed we find CO to be poorly correlated with HI and thermal radio continuum emission as well.

3.2.2. Estimate of total CO content of NGC 6822

We have coadded the spectra from all observed positions, with *equal weight for each position*, in order to obtain an impression of what the total CO spectrum of NGC 6822 as a whole might look like. Since part of the sample was observed with the high-resolution backend (HRS) only, we constructed spectra for both the low-resolution and the high-resolution data separately. Because some of the survey beams overlapped, the actual surface area covered in terms of beams is less than the number of positions observed. The resulting spectrum has been published, in a different context, by Israel, Tacconi & Baas (1995). The numerical results are, however, included in Table 1. The velocity-integrated CO strength obtained for all positions together is about 70 per cent greater than the sum of the six detections and marginal detections. This implies an *average* contribution of $\int T_{mb} dV = 0.2$ K km s^{-1} from each of the eleven nondetections, below the individual detection limits, indicating the presence of very weak CO emission beyond the positions detected.

Because of the good correlation between CO and far-infrared intensities, we may take the latter as indicative for the probable extent of CO emission, implying that we have covered 8 per cent of the surface of NGC 6822 in the low-resolution observations and 14 per cent in the high-resolution observations. The *observed* summed CO luminosity of NGC 6822 is $\int T_{mb} dV\ dA = 5.4 \pm 1.0 \times 10^4$ K km s^{-1} pc^2 (HRS observations). To this, one might add another $1.1 \pm 0.2 \times 10^4$ K km s^{-1} pc^2 from the two detections by W92 not in common with ours. If the fraction of NGC 6822 sampled in CO is representative for the remainder of the galaxy, the total CO luminosity would be six times higher, *i.e.* $\int T_{mb} dV\ dA = 4 \pm 1 \times 10^5$ K km s^{-1} pc^2. We consider this an upper limit, for the following reasons. *i.* Our survey, as well as the one by W92, was biased towards positions where CO was considered to be most likely detectable. *ii.* The increase in coverage from LRS to HRS observations does not yield a commensurate increase in CO luminosity. *iii.* The W92 observations cover a larger surface area than our survey; the W92 detection sum, divided by the fraction of the galaxy covered, yields a total CO luminosity of $1.7 \pm 0.7 \times 10^5$ K km s^{-1} pc^2, only 2.5 times higher than detected. *iv.* Since CO is detected primarily towards the brighter IR sources, the low infrared surface brightness of the remaining areas not covered suggests that only weak CO emission will be present there. If we simply scale the CO by FIR luminosity, or if we extrapolate the I_{CO}/FIR′ relation from the Sect. 3.2.1 to the total FIR luminosity of NGC 6822, we obtain a total CO luminosity only 1.5 times higher than the detected CO luminosity .

As the best estimate based on these considerations, we adopt an *extrapolated total CO luminosity* $\int T_{mb} dV\ dA = 1.2$ (+1.2, -0.6) $\times 10^5$ K km s^{-1} pc^2. This is twice the detected luminosity; the lower and upper limits correspond to the luminosities detected and maximum extrapolated from the W92 observations respectively.

4. Discussion

4.1. Is the Galactic value of X = N(H_2/I_{CO}) applicable to NGC 6822?

If we were to assume a CO to H_2 conversion factor equal to the 'standard' Galactic conversion factor, i.e. N(H_2) = 2.0 $\times$ 10^{20} $\int T_{mb} dV$ cm^{-2} (Bloemen 1989), the above would imply an H_2 mass M(H_2) = 4 (+4, -2) $\times$ 10^5 $M_\odot$, less than one per cent of the HI mass of NGC 6822. Towards the sources actually detected, the N(H_2)/N(HI) ratio would be no more than a few per cent.

However, it is questionable whether the 'standard' Galactic conversion applies to a dwarf galaxy like NGC 6822 with rather different conditions prevalent in its interstellar medium. Three observations suggest that indeed a rather higher conversion factor applies to NGC 6822, leading to much higher H_2 masses.

Firstly, the CO luminosities of the three narrow-line sources are lower by a factor of 30 than those of Galactic clouds with the same linewidths (Dame et al. 1986) and by a factor of six or more than those in the LMC (Cohen et al. 1988, Garay et al. 1993). Since the three sources with wider lines have luminosities similar to the narrow-line sources, they appear at first glance to be even more extreme. However, they may be extended beyond the observing beam, or the greater linewidths may represent superposition of different clouds in the line of sight. In that case, the broad-line clouds may in fact conform to the narrow-line sources. Nevertheless, the observations of NGC 6822 clearly indicate its CO clouds to be strongly subliminous for their linewidth, in comparison not only with the galaxy, but even with the LMC.

Secondly, the mass of new stars formed in NGC 6822 over the last 10^7 years is of the order of 4 $\times$ 10^5 $M_\odot$ Paper I). The low H_2 mass estimates would thus indicate rather high recent star formation efficiencies of 50$\pm$17 % *galaxy-wide*, which we consider unlikely.

Thirdly, CO is detected towards positions where the far-infrared is enhanced by factors of 5 to 10 with respect to the surroundings, yet without commensurate increase in HI column density (Hubble X being the exception). If we were to explain the infrared enhancements not by the presence of significant local dust and molecular gas masses, but by higher dust temperatures, the infrared sources should have temperatures 40 - 50% higher than the surrounding extended dust, i.e. 40 - 45 K. As this implies 60/100μm flux ratios of unity, completely ruled out by the observations presented in Paper I, we must reject this explanation.

4.2. An estimate of X_{N6822} and the H_2 mass of NGC 6822

The last observation suggests a way of estimating the actual value of X, the ratio of molecular hydrogen column density N(H_2) to velocity-integrated CO strength I_{CO} in NGC 6822. Because of the difficulty of arriving at a specific value for X, we first present a rather conservative derivation yielding a *firm* lower limit for X, which nevertheless is already substantially higher than X_{Gal}. We then discuss the systematic effects that cause the derived value of X to be a *lower limit* and arrive at a probable, but less firm final value of X_{N6822}.

The HI map published by Gottesmann & Weliachew (1977) and the maps in Paper I show that well away from the major HI and infrared peaks, a far-infrared surface brightness of 7.6 $\times$ 10^{-8} W m^{-2} sr^{-1}, implying a far-infrared intensity of 2.7 $\times$ 10^{-14} W m^{-2} in the 2.3′ HI beam, corresponds to a column density N(HI) = 10^{21} cm^{-2}. In order to determine the value of X_{N6822} we make the following assumptions. First, we assume that at these positions molecular emission is nil, so that N_H/FIR = (N(HI)/FIR)$_\circ$ = 3.75 $\times$ 10^{34} cm^{-2} W^{-1} m^2. Second, we assume that the gas-to-dust ratio is constant throughout, which is a reasonable assumption for NGC 6822 (*cf.* Vila-Costas & Edmunds (1992; their Fig. 1e). Third, we assume that the temperature distribution of radiating dust is the same at positions with and without CO, so that FIR values reduced to the same temperature correctly measure dust column densities. Because derived dust temperatures vary only little over all of NGC 6822, irrespective of infrared intensity (Paper I), this is also a reasonable supposition.

Under these assumptions, the ratio N_H/FIR is a measure for the total gas-to-dust ratio, independent of the form (atomic or molecular) in which the gas is present and should be constant throughout NGC 6822. As we show below, departures from these assumptions will only lead to higher values of X. At positions where CO has been detected, associated H_2 should be present with a column density N(H_2) = 0.5 $\times$ (N_H - N(HI)), where the righthand side of the equation now contains known quantities. A value for X thus follows from this H_2 column density and the observed I_{CO}:

$$X_{N6822} = N(H_2)/I_{CO} =$$

$$0.5 \times [(3.75\ 10^{34}\ f(T_d)\ FIR) - N(HI)]\ I_{CO}{}^{-1}$$

Here, FIR is the observed infrared luminosity in W m^{-2}, f(T_d) is a function close, but not identical to (28.5/T_d)^6, where T_d is the derived dust temperature for n = 2 (*cf.* Table 2 and discussion in Paper I), N(HI) is the HI column density in cm^{-2} from the map by Gottesman & Weliachew (1977) and I_{CO} in K km s^{-1} is the integrated CO strength from Table 1. The temperature term corrects, to first order, for the strong temperature dependence of the dust infrared emissivity. This is sufficient, because temperatures T_d vary less than 10% over NGC 6822, so that f(T_d) varies by no more than a factor 1.6. In Table 3 we list the relevant observed values, and the resulting values for X. For comparison, we also include the CO results from W92; Hubble V is the only detection in common.

In Table 3, the values for X are remarkably consistent; the mean is X_{N6822} = 4.5$\pm$0.7 $\times$ 10^{21} cm^{-2} (K km s^{-1})$^{-1}$ = 23$\pm$4 X_{Gal} (*cf.* Bloemen (1989). The values derived from the W92 CO data are somewhat higher; inclusion into the total yields a mean X_{N6822} = 5.2$\pm$0.5 $\times$ 10^{21} cm^{-2} (K km s^{-1})$^{-1}$ or 26$\pm$3 X_{Gal}. Thus, the CO to N(H_2) conversion factor applicable to NGC 6822 is *at least* a factor of 20 higher than in the Galaxy. The high value follows directly from the weakness of the observed

Table 3. Lower limits to X = $N(H_2)/I_{CO}$ for NGC 6822 positions

Object	CO Position	$\int T_b(CO)dV$ (K km s^{-1})	N(HI)[a] 10^{21} (cm^{-2})	FIR[b] 10^{-13} (W m^{-2})	$f(T_d)$[c]	X[d] 10^{20} (cm^{-2} K^{-1} km^{-1} s)
HubbleI	1	0.39±0.12	1.45	2.1	0.74	56±17
IR#4	5	0.80±0.14	1.75	2.3	0.90	38±7
HubbleV	7	0.77±0.07	1.15	4.7	0.55	56±5
IR#6	12	0.90±0.16	1.15	2.9	0.67	34±6
HubbleX[e]		0.34±0.11	2.90	2.1	0.82	52±17
HubbleV[e]		0.71±0.16	1.15	4.7	0.55	60±14
SW-HI Peak[e]		0.43±0.11	1.75	2.3	0.90	70±18

Notes to Table 3: (a): From Gottesman & Weliachew 1977; (b): From Paper I; (c): Assumed reference temperature for diffusely distributed dust T_d = 28.5 K; see Sect. 4.2, point (iii). (d): Errors in X are those due to uncertainties in I_{CO} only; (d): CO data taken from W92 converted to T_{mb}.

CO emission on the hand, and the relatively high far-infrared intensities at those positions where CO is detected. As noted before, the above result is a lower limit; the systematic effects discussed below can only increase the value of X.

(i). Our null-assumption may be wrong, and some CO emission may be present where we assumed none. In that case, we have underestimated the total hydrogen column density corresponding to unit infrared luminosity, and X will be higher than derived above. For instance, if there were a contribution I_{CO} = 0.1 K km s^{-1} per beam area where we assumed nil, we would find a 20% higher value for X. It is easily seen that the presence of H_2 uncontaminated by CO would have the same effect.

(ii). The infrared source luminosities in Paper I (and Table 3) are corrected for the contribution from extended diffuse emission in NGC 6822. However, the HI column densities sample both source and extended emission. If we add to the source infrared luminosities the contribution from the extended emission in a 2.3′ beam, we find higher total hydrogen column densities N_H with unchanged HI column densities N(HI), leading to an increase in the mean value of X by 30%.

(iii). The observed infrared source luminosities are reduced to the temperature of the dust responsible for the extended far-infrared emission. For this we took the lowest value compatible with the infrared data (T_d = 28.5 K if n = 2; $f_{60\mu}/f_{100\mu}$ = 0.40). In fact, the extended emission has a *higher* nominal temperature: the data imply $f_{60\mu}/f_{100\mu}$ = 0.47 corresponding to T_d = 30 K. Insertion of that temperature again leads to an increase in X, by 50%. Note that X values close to X_{Gal} are only obtained if the reference dust temperature T_d were as low as 24 K. The corresponding flux ratio $f_{60\mu}/f_{100\mu}$ = 0.25 is completely ruled by the data presented in Paper I. Because the derived temperatures cover only a narrow range over all of NGC 6822, the result is largely independent of the assumed value n of the wavelength dependence of the dust emissivity, and also largely independent of uncertainties in the temperature derivation. The possible presence of cooler dust hidden by the higher emissivity of the warmer dust sources (for instance Hubble V) would also lead to higher X values.

(iv). Because CO emission is observed primarily from regions bright in the infrared, the relatively strong radiation field densities implied by the latter may have caused depletion of dust in these regions. They would then have a higher gas-to-dust ratio than their surroundings, invalidating our assumption that the gas-to-dust ratio is the same everywhere. In that case, however, we would have underestimated the total hydrogen column-density, once again leading to a higher value of X.

(v). The FIR to N_H ratio derived above corresponds to a dust-to-gas ratio of 2×10^{-4}, i.e. one and a half times the value obtained from global galaxy fluxes. This is not unreasonable, because the total HI mass resulted from integration over a larger area than could be used to obtain the integrated infrared emission. If we were to accept the lower dust-to-gas ratio as representative, the same amount of infrared emission would imply a higher total hydrogen column density and a value for X about 50% higher.

(vi). The CO emission is measured in a 43″ beam, while the infrared sources were sampled with a resolution of about 1′ (Paper I). If the extent of the observed CO emission is small compared to the SEST beam, I_{CO} would be lower in the larger 1′ beam by a factor up to two, which would increase the derived X value by that same factor. In this context, the 30% larger value for X implied by the CO observations in the larger W92 beam is perhaps significant. As a further check, we also derived X using the *average* values given in Table 1 which represent larger areas. This yields a mean value $X_{N6822} = 6.7\pm1.4 \times 10^{21}$ cm^{-2} (K km $s^{-1})^{-1}$ = 33±7 X_{Gal}, or 45±12 % higher.

Thus, any of these attempts to make the calculation more realistic results in a noticeably higher value of X. The systematic effects discussed, and their magnitude, leads us to conclude that *a more realistic value is* $X_{N6822} = 8\pm3 \times 10^{21}$ cm^{-2} = *40±15* X_{Gal}. Other authors have also suggested very high values for X in dwarf galaxies (*cf.* Verter & Hodge 1995 and references therein). The explanation for such high values of X is not immediately clear. Low metallicities in combination with strong UV radiation fields will allow selective depletion of CO with respect to H_2. Thus, only a small fraction of the H_2 volume will be filled with CO, most likely in the form of small, dense clouds. Alternatively, a lack of cosmic ray particles, consistent with the weak nonthermal emission from NGC 6822 (Klein et al. 1983; see also Paper I), might cause poor excitation of CO resulting

in excitation temperatures lower than in the Galaxy, and also result in weaker CO emission. We note that the value for X_{N6822} derived here agrees well with a proposed correlation of X with metallicity (*cf.* Fig. 2 in Verter & Hodge 1995). It is also more than a magnitude greater than the value of X obtained interferometrically for CO clouds in Hubble V (Wilson, 1994). Again, this fits a trend discussed by Verter & Hodge (1995) and illustrated in their Fig. 2, which shows that X values derived from measurements with large linear beamsizes ($\geq$ 100 pc, such as ours) are generally much higher than those derived by using small linear beamsizes ($\leq$ 50 pc, such as used by Wilson 1994). We will return to Hubble V in a later paper.

We may use our value of X to predict the expected integrated CO brightness at the positions of the infrared sources not detected in CO. The resulting average brightness is I_{CO} = 0.2 K km s^{-1}, which is in fact identical to the average brightness of 'nondetected' positions deduced in Sect. 4.2. Taking $X_{N6822} = 40\pm15\ X_{Gal}$, the CO content of NGC 6822 estimated in Sect. 3.2.2 corresponds to a molecular hydrogen mass $M(H_2)$ = 1.5 (+3, -1) $\times$ 10^7 $M_\odot$, implying a molecular gas fraction $M(H_2)/M(H_2+HI+He)$ = 0.10 (+0.13,-0.06). Although the actual molecular hydrogen mass in NGC 6822 is substantially in excess of what one would predict from the observed low CO brightness and the Galactic CO-to-H_2 conversion, it is at most 45% of the atomic hydrogen mass, and more likely about 15% of this.

5. Conclusions

1. CO was searched for in 17 positions, and detected clearly in four and marginally in two. Where detected, CO emission is invariably weak. All CO detections are towards positions of relatively strong infrared emission; CO brightnesses correlate well with far-infrared brightness.
2. Analysis suggests that the whole body of NGC 6822 does not produce more than a few times the amount of detected CO emission. Comparison of CO, HI and far-infrared emission suggests that in NGC 6822 the $N(H_2)/I_{CO}$ ratio is 40 ± 15 times higher than in the Galaxy, with $X_{N6822} = 8\pm3 \times 10^{21}$ cm^{-2} (K km $s^{-2})^{-1}$. This may reflect small CO filling factors of H_2 clouds, low CO excitation temperatures or both.
3. With this conversion factor, NGC 6822 contains a mass of molecular hydrogen of $M(H_2)$ = 1.5 (+3, -1) $\times$ 10^7 $M_\odot$, implying that about 10% (at most 25%) of the interstellar medium in the galaxy is in molecular form.

Acknowledgements. It is a pleasure to thank the operating personnel of the SEST for their support. I am also grateful to Frank Helmich and Jan Lub for assistance with the SEST-CO observations.

References

Bloemen J.B.G.M., 1989 in *Physics and Chemistry of Interstellar Molecular Clouds*, Lecture Notes in Physics, Vol 331, Eds. G. Winnewisser& J.T. Armstrong (Berlin: Springer), p. 22
Cohen R.S., Dame T.M., Garay G., Montani J., Rubio M., Thaddeus P., 1988 *ApJL*331, L95
Dame T.M., Elmegreen B.G., Cohen R.S., Thaddeus P., 1986 *ApJ* 305, 892
Dufour R.J., 1984 in *Structure and Evolution of the Magellanic Clouds*, IAU Symp. 108, Eds. S. van den Bergh and K.S. de Boer (Dordrecht: Kluwer), p. 353
Elmegreen B.G., Elmegreen D.M., Morris M., 1980 *ApJ* 240, 455
Fisher J.R., Tully R.B., 1975 *A&A* 44, 151
Gallagher J.S., Hunter D.A., Gillett F.C., Rice W.L., 1991 *ApJ* 371, 142
Garay G., Rubio M., Ramírez S., Johansson L.E.B., Thaddeus P., 1993 *A&A* 274, 743
Gottesman S.T., Weliachew L., 1977 *A&A* 61, 523
Gredel R., van Dishoeck E.F., de Vries C.P., Black J.H., 1992 *A&A* 257, 245
Gredel R., van Dishoeck E.F., Black J.H., 1994 *A&A* 285, 300
Hartmann D., 1994 Ph.D. thesis Leiden University
Hodge P.W., 1977 *ApJS*33, 69
Hodge P.W., 1980 *ApJ* 241, 125
Hodge P.W., Kennicutt R.C., Lee M.G., 1988 *PASP* 100, 917
Hubble E., 1925 *ApJ* 62, 409
Humphreys R.M., 1980 *ApJ* 238, 65
Israel F.P., Tacconi L.J., Baas F., 1995 *A&A* 295, 599
Israel F.P., Bontekoe Tj. R., Kester D.J.M., 1995 *A&A* in press (Paper I)
Klein U., Gräve R., Wielebinski R., 1983 *A&A* 117, 332
Lequeux J., Peimbert M., Rayo J.F., Serrano A., Torres-Peimbert S., 1979 *A&A* 80, 155
McAlary C.W., Madore B.F., McGonegal R., McLaren R.A., Welch D.L., 1983 *ApJ* 273, 539
Ohta K., Tomita A., Saito M., Sasaki M., 1993 *PASJ* 45, L21
Pagel B.E.J., Edmunds M.G., Smith G., 1980 *MNRAS* 193, 219
Skillman E.D., Terlevich R., Melnick J., 1989 *MNRAS* 240, 563
Stark R., 1993 Ph.D. Thesis, Leiden University
Vangioni-Flam E., Lequeux J., Maucherat-Joubert M., Rocca-Volmerange B., 1980 *A&A* 90, 73
Verter F., Hodge P.W., 1995 *ApJ* 446, 616
Vila-Costas M.B., Edmunds M.G., 1992 *MNRAS* 259, 121
Volders L., Högbom J.A., 1961 *BAN* 15, 307
Wilson C.D., 1992a *ApJ* 391, 144 (W92)
Wilson C.D., 1992b *AJ* 104, 1374
Wilson C.D., 1994 *ApJL*434, L11

This article was processed by the author using Springer-Verlag LaTeX A&A style file *L-AA* version 3.